

PILOT: Efficient Planning by Imitation Learning and Optimisation for Safe Autonomous Driving

Henry Pulver*, Francisco Eiras*[†], Ludovico Carozza*, Majd Hawasly*,
Stefano V. Albrecht*[‡] and Subramanian Ramamoorthy*[‡]

*FiveAI Ltd., United Kingdom

Email: first.last@five.ai

[†]University of Oxford, United Kingdom

[‡]University of Edinburgh, United Kingdom

Abstract— Achieving the right balance between planning quality, safety and runtime efficiency is a major challenge for autonomous driving research. Optimisation-based planners are typically capable of producing high-quality, safe plans, but at the cost of efficiency. We present PILOT, a two-stage planning framework comprising an imitation neural network and an efficient optimisation component that guarantees the satisfaction of requirements of safety and comfort. The neural network is trained to imitate an expensive-to-run optimisation-based planning system with the same objective as the efficient optimisation component of PILOT. We demonstrate in simulated autonomous driving experiments that the proposed framework achieves a significant reduction in runtime when compared to the optimisation-based expert it imitates, without sacrificing the planning quality.

I. INTRODUCTION

Guaranteeing safety of decision-making is a fundamental challenge in the path towards the long-anticipated adoption of autonomous vehicle technology. Attempts to address this challenge show the diversity of possible definitions of what safety means: whether it is maintaining the autonomous system inside a safe subset of possible future states [1], [2], preventing the system from breaking domain-specific constraints [3], [4], or exhibiting behaviours that match the safe behaviour of an expert [5], amongst others.

Typically, model-based approaches to safety are engineering-heavy and require deep knowledge of the application domain. On the other hand, the hands-off aspect of data-driven approaches is lucrative, which is evidenced by the growing interest in the research community in exploiting techniques like imitation learning for autonomous driving [6], [7], [8], [9].

Moreover, inference using a data-driven model is usually very efficient compared to more elaborate search- or optimisation-based approaches. On the other hand, model-based planning approaches give a better handle on understanding system expectations through model specification and produce more interpretable plans [10], [11], [12], but usually at the cost of robustness [3] or runtime efficiency [4].

As is well known to practitioners, a simplistic attempt to leveraging learning from data in this setting (e.g. a vanilla behavioural cloning approach to imitation learning [13]), will likely fail to exhibit safe behaviour at deployment time due to covariate shift between the situations in the specific expert



Fig. 1. An example CARLA simulation, showing in red the trace of an expensive-to-run planner (2s-OPT) that took 175 ms on average for a planning horizon of 8 seconds, and PILOT’s trace in blue that took 44 ms for the same planning horizon.

training data and the deployment environment [14], [15], even with a prohibitive amount of training data. Attempts to improve deployment time performance include online augmentation that actively enriches the training data with actual experiences of the learner in the deployment environment [16], and offline approaches that synthesise realistic perturbed instances from the expert dataset to include more failure cases and near-misses [17].

Still, pure data-driven approaches struggle in practice to certify the safety of their output at deployment time without major investments in robust training [18], [19] or post-hoc analysis [20], especially in a safety-critical application like autonomous driving. Thus, hybrid approaches that leverage model-based components to give safety guarantees on the output of a data-driven system have emerged [21], e.g., using control safe sets to validate acceleration and steering commands predicted by a neural network [22].

In this work, we embrace a hybrid approach to imitation learning from data, but instead of depending on curated, human expert data in the learning scheme, we imitate traces generated by a performant optimisation-based planner that is expensive-to-run. We train a neural planner that is much more efficient than the expert planner but maintains its standard of planning quality. To guarantee the safety of the output of the system we employ an efficient optimisation step that uses the same objective function as the expert but benefits from the network output as a warm-start.

This imitation learning paradigm does not introduce any superficial limitations to the sophistication of the system

specification. This is in contrast to approaches such as Constrained Policy Nets [23] in which the cost function of an optimisation-based planner is made into a loss function to train a policy network from scratch, requiring careful treatment of the constraint set.

Without loss of generality to our approach, in this paper we use the two-stage optimisation approach in [4] as the expensive-to-run planner to imitate. We use an in-the-loop Dataset Aggregation (DAgger) [16] approach to imitation learning to train a deep neural network to imitate the output of the expert planner. The online augmentation using DAgger benefits from the fact that the expert planner is always available to update the training dataset. This reduces the training cost compared to using human expert data, and targets the augmentation compared to other dataset augmentation techniques that rely on random perturbations to the expert problems, e.g. [22], [24].

We demonstrate the performance of our imitation learning and optimisation architecture, called **PILOT** – *Planning by Imitation Learning and Optimisation* – on sets of simulated experiments generated using a light-weight simulator and using CARLA [25]. We show that PILOT leads to a much improved running time when compared to the expensive-to-run planner (a reduction of around 80% in our experiments), at no significant loss in the solution quality, measured by the cost of the objective function of the final trajectory.

The contributions of this work are:

- A robust and scalable deep learning framework to imitate an expensive-to-run optimiser, rectified by an efficient optimiser with the same cost function as the expert.
- Application of this framework to the two-stage optimisation-based planner [4], leading to a runtime improvement of around 80% in our benchmark datasets.

II. PILOT: PLANNING BY IMITATION LEARNING AND OPTIMISATION

We introduce PILOT, our solution to improve the efficiency of expensive-to-run optimisation-based planners. For any variable v_j with $j \in \mathbb{R}^+$, we will use the shorthand $v_{i:e} = \{v_i, \dots, v_e\}$. We assume the input to the planning problem to be given by the scene $s \in \mathbb{R}^S$ (e.g. including vehicle states, layout information, predictions of other agents), and the goal is to obtain a plan for the *ego-vehicle* (abbreviated to ego for brevity) as a sequence of N states: $\tau^* = \tau_{1:N} \in \mathbb{R}^{Nd}$ such that it optimises:

$$\begin{aligned} \operatorname{argmin}_{\tau} \quad & \mathcal{J}(\tau) \\ \text{s.t.} \quad & \tau_1 = s_{\text{ego}}, \quad g_s(\tau) \leq 0, \quad h_s(\tau) = 0 \end{aligned} \quad (1)$$

where \mathcal{J} is a cost function defined over the plan, s_{ego} refers to the initial ego state given s , $g_s = (g_s^1, \dots, g_s^L)$ and $h_s = (h_s^1, \dots, h_s^M)$ are possibly nonlinear, non-convex, inequality and equality constraints, respectively, on the ego-vehicle states parameterised by the input scene. As is well known in the community, while globally solving this optimisation problem is NP-hard [26], [27], there are in practice efficient

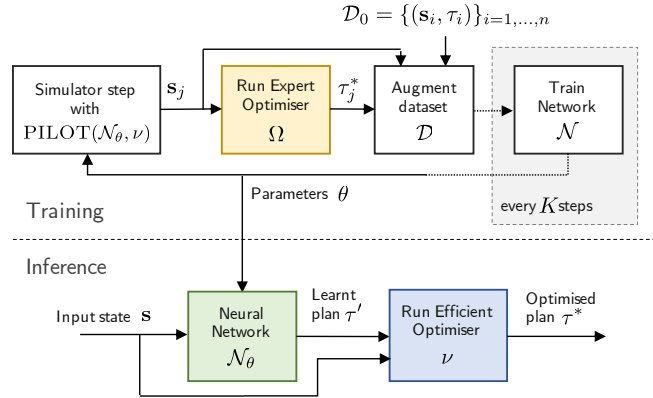


Fig. 2. PILOT framework: PILOT uses an expert-in-the-loop imitation learning paradigm to train a deep neural network, \mathcal{N}_θ , that imitates the output of the expensive-to-run optimisation-based planner Ω (top). At inference time, it uses the output of \mathcal{N}_θ to initialise an efficient optimiser ν to compute a feasible and low cost trajectory (bottom).

solvers that compute local solutions within acceptable times assuming a sensible initial guess is provided [28], [29]. We define ν to be such an *efficient optimiser* that solves Eq. 1 (e.g., [28]), and Ω to be the ‘expert’ *expensive-to-run optimisation* procedure that attempts to improve upon the local optimum of Eq. 1 found by ν . Examples of Ω can include performing a recursive decomposition of the problem and taking the minimum cost [30], or applying other warm-starting procedures [4], [31].

The goal of PILOT is to safely achieve low costs on \mathcal{J} , comparable to the safe levels achievable by Ω , but in runtimes comparable to the efficient ν . To do so, PILOT employs an imitation learning paradigm to train a deep neural network \mathcal{N}_θ to imitate the output of Ω , which it then uses to initialise ν in order to output a feasible trajectory that maintains the safety and smoothness guarantees provided by the constraints. This is shown in Algorithm 2 and Fig. 2 (bottom).

In order to achieve that, we pre-train the network on a dataset of problems labelled by the expert planner, $\mathcal{D}_0 = \{(\mathbf{s}_i, \tau_i)\}_{i=1,\dots,n}$. Then, using the pre-trained \mathcal{N}_θ augmented with ν as the planner in a simulator, we employ a DAgger-style training loop [16] to adapt to the covariate shift between the training dataset \mathcal{D}_0 and the learner’s experience in the simulator. For more details, see Algorithm 1 and Fig. 2 (top).

III. PILOT FOR THE TWO-STAGE OPTIMISATION-BASED MOTION PLANNER

For the sake of demonstration, we use the two-stage optimisation-based planning framework introduced by Eiras *et al.* [4] as Ω to showcase PILOT.

A. Two-stage Optimisation-based Motion Planner

Fig 3(a) and (b) show the architecture of the two-stage optimiser which we will refer to as 2s-OPT in this paper. The input to the system are: 1) a birds-eye view of the planning situation, that includes the ego vehicle, other road users and the relevant features of the static layout; 2) a route plan as a reference path, provided by an external

Algorithm 1: PILOT TRAINING PROCEDURE

input : initial dataset $\mathcal{D}_0 = \{(\mathbf{s}_i, \tau_i)\}_{i=1, \dots, n}$,
 expensive-to-run planner Ω , efficient planner ν , simulator \mathcal{S} , training problems count J
output: trained network parameters θ
 Initialise \mathcal{D} to \mathcal{D}_0
 Pre-train $\theta \leftarrow \text{TRAIN}(\mathcal{N}, \mathcal{D})$
for $j \in \{n + 1, \dots, J\}$ **do**
 | **if** simulation finished **then**
 | | $\mathbf{s}' \leftarrow$ Initialise a new simulation
 | **else**
 | | $\mathbf{s}' \leftarrow \mathbf{s}_{j-1}$
 | | Obtain \mathbf{s}_j by stepping in \mathcal{S} with
 | | PILOT($\mathbf{s}'; \mathcal{N}_\theta, \nu$)
 | | Get τ_j^* by optimising \mathcal{J} using $\Omega(\mathbf{s}_j)$
 | | Update $\mathcal{D} \leftarrow \mathcal{D} \cup \{(\mathbf{s}_j, \tau_j^*)\}$
 | | // retrain network every K steps
 | **if** $j \bmod K = 0$ **then**
 | | Update $\theta \leftarrow \text{TRAIN}(\mathcal{N}, \mathcal{D})$
return θ

route planner; and 3) predicted traces for all road users, provided by a prediction module. Projecting the world state and predictions into a reference path-based coordinate frame produces 2s-OPT input (Fig 3(a), for more details see [4]).

We define Δt to be the timestep between states, N the desired plan length, and the discretised kinematic bicycle model $\mathbf{x}_{k+1} = f_{\Delta t}(\mathbf{x}_k, \mathbf{u}_k)$, where \mathbf{x}_k is ego state and \mathbf{u}_k is control (acceleration and steering) applied to the ego at step k . The goal of the 2s-OPT framework is to solve the following optimisation problem:

$$\begin{aligned} \operatorname{argmin}_{\mathbf{x}_{1:N}, \mathbf{u}_{0:N-1}} \quad & \mathcal{J}(\mathbf{x}_{1:N}, \mathbf{u}_{0:N-1}) \\ \text{s.t.} \quad & \mathbf{x}_{k+1} = f_{\Delta t}(\mathbf{x}_k, \mathbf{u}_k) \\ & \mathcal{E}(\mathbf{x}_k) \cap ([\mathbb{R}^2 \setminus \mathcal{B}] \cup \mathcal{S}_k^{1:w}) = \emptyset, \forall k \end{aligned} \quad (2)$$

where $\mathcal{B} \subset \mathbb{R}^2$ is the driveable surface that is safe to drive based on the layout, $\mathcal{S}_{1:N}^{1:w} \subset \mathbb{R}^{2 \times N}$ are unions of elliptical areas that encompass the w road users, $\mathcal{S}_k^{1:w}$, for timesteps $k \in \{1, \dots, N\}$, $\mathcal{E}(\mathbf{x}_k) \subset \mathbb{R}^2$ is the area the ego occupies at step k with, and \mathcal{J} is a cost function comprising a linear combination of quadratic terms of comfort (reduced acceleration and jerk) and progress (longitudinal and lateral tracking of the reference path, as well as speed) [4]. In 2s-OPT, the authors approximate the ego's area $\mathcal{E}(\mathbf{x}_k)$ by its corners, so that the intersection with the driveable surface – delimited by its borders which are defined as C^2 functions – and road user ellipses can be computed in closed form [4].

To solve this problem, the authors apply the two-stage architecture presented in Fig 3(b). The first stage solves a linearised version of the planning problem using a Mixed-Integer Linear Programming (MILP) solver. The output of the MILP solver is fed as a warm-start initialisation to the NLP optimiser. This second optimisation stage ensures that the output trajectory is smooth and feasible, while

Algorithm 2: PILOT INFERENCE STEP

input : state \mathbf{s} , trained imitation network \mathcal{N}_θ ,
 efficient planner ν
output: optimal plan τ^*
 Obtain initial trajectory $\tau' \leftarrow \mathcal{N}_\theta(\mathbf{s})$
 Get τ^* by optimising \mathcal{J} using $\nu(\mathbf{s}, \tau')$
return τ^*

maintaining safety guarantees. For more details, the reader is referred to [4].

As discussed by the authors [4], although the framework produces superior outputs when compared to alternatives with regard to solution quality (measured by convergence guarantee and output cost values), it suffers from the typical limitation of pure optimisation approaches in solving time, as the method effectively trades off efficiency for better solution quality.

B. PILOT for 2s-OPT

In this section we describe how PILOT could be used with 2s-OPT as the expert expensive-to-run planner Ω . We design a convolutional neural network $\mathcal{N}_\theta^{2s\text{-OPT}}$ to take as input a graphical representation of the scene (including predictions of other road users) in addition to other scalar parameters of the problem (e.g. speed of the ego vehicle), and to output a smooth trajectory. We train $\mathcal{N}_\theta^{2s\text{-OPT}}$ using Algorithm 1 to imitate the output of 2s-OPT when presented with the same planning problem. For the efficient optimisation planner ν , we use the NLP constrained optimisation stage from 2s-OPT. In the next subsections we describe the input and output representations of $\mathcal{N}_\theta^{2s\text{-OPT}}$, as well as the training procedure.

1) Pre-processing and input representation: The planning scene \mathbf{s} comprises the static road layout, road users with their predicted trajectories, and a reference path to follow. As the problem is transformed to the reference path coordinate frame, the resulting scene is automatically aligned with the area of interest – the road along the reference path (see Fig. 3(a)), simplifying the network representation.

To encode the predicted trajectories of dynamic road users, C greyscale top-down images of the scene $I_t^s \in \mathbb{R}^{W \times H}$ are produced by sampling the positions of road users along their predicted trajectories uniformly at times $t \in \{0, \frac{h}{C-1}, \dots, h\}$, for the planning horizon $h = N\Delta t$. These images create an input vector $\mathcal{I}^s = I_{1:C}^s \in \mathbb{R}^{C \times W \times H}$, which is then fed into convolutional layers that extract semantic features, as shown in Fig. 3(c). This is similar to the input representation in previous works, e.g. ChauffeurNet [17], with the exception that in our case the static layout information is repeated on all channels.

Additional information of the planning problem that is not visualised in the top-down images (such as the initial speed of the ego vehicle) is appended as scalar inputs, along with the flattened convolutional neural network (CNN) output, to the first dense layer of the network. We refer the reader to Appendix A more details.

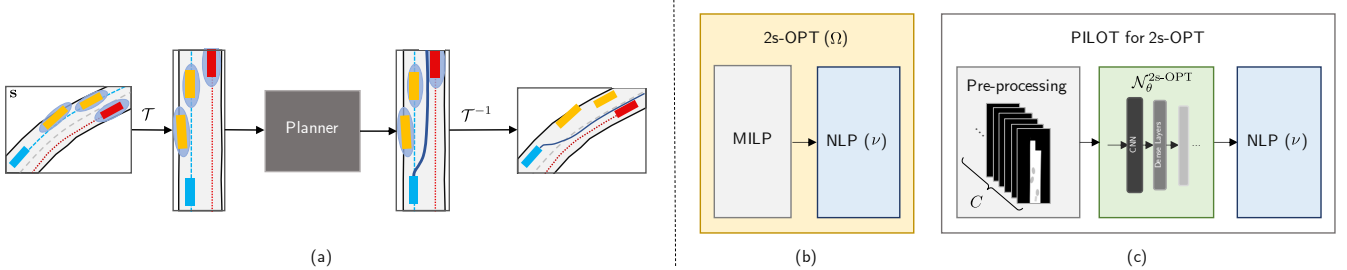


Fig. 3. PILOT for 2s-OPT: (a) The planning input state is first transformed from the global coordinate frame to the reference path-based coordinate frame. After the plan is obtained, the output is transformed back to the global coordinate frame by the inverse transform. See [4] for more details; (b) Architecture of 2s-OPT (expert, expensive-to-run planner Ω): a Mixed-Integer Linear Programming problem initialises an NLP problem; (c) Architecture of PILOT for 2s-OPT: input pre-processing produces a sequence of images of the scene, encoding road surface information and the predicted future of dynamic road users, the network $\mathcal{N}_\theta^{2s\text{-OPT}}$ which was specifically designed for this problem, and the NLP problem as in 2s-OPT (ν).

2) *Network training and output representation*: The output of the network is a trajectory in the reference path coordinate frame. One possibility is to output a vector $\rho^\theta \in \mathbb{R}^{2 \times N}$, encoding time-stamped positions, i.e., $\rho^\theta = \{(x_j, y_j)\}_{j=1, \dots, N}$. Using such a representation, we can define the training loss to be the L_2 norm between the expert trajectory and the network output:

$$\mathcal{L}_\theta(\mathcal{D}) = \frac{1}{nN} \sum_{i \in \mathcal{D}} \|\rho_i^\theta - \rho_i^*\|^2 + \mu \|\theta\|^2, \quad (3)$$

where θ refers to the neural network parameter vector, \mathcal{D} is the dataset of training examples, and ρ_i^* indicates the expert's time-stamped positions at index i from the dataset.

To enforce smoothness in the output, an alternative is to train the network to produce parameters of a smooth function family over time which can then be sampled to obtain ρ . Let us assume that $x_{1:N}$ can be parameterised as a function of its index j by a parametric C^1 function \mathcal{F}^x with parameters \mathbf{p}_x , and similarly for $y_{1:N}$ with \mathcal{F}^y and parameters \mathbf{p}_y , i.e.:

$$x_j = \mathcal{F}^x(j; \mathbf{p}_x), \quad y_j = \mathcal{F}^y(j; \mathbf{p}_y)$$

In this case, the gradients of \mathcal{F}^x and \mathcal{F}^y can be computed analytically, and can thus consider this to be an extra layer of the network (with fixed weights and an appropriate choice of activation function) and maintain the loss definition in Eq. 3. Examples of the parametric functions that satisfy the requirements could be polynomials or B-splines. In cases where \mathbf{p}_x and \mathbf{p}_y have hyperparameters (e.g. the degree of a polynomial), we can determine their optimal values by performing cross-validation in our training dataset.

The efficient NLP optimisation planner (detailed in Sec. III-A) expects as initialisation a time-stamped sequence of positions, speeds, orientations and control inputs (steering and acceleration), all in the reference path coordinate frame. We calculate speeds and orientations from the sequence of points produced by the network, and derive control inputs from the inverse dynamics model.

IV. EXPERIMENTS

In this section, we show results comparing PILOT and 2s-OPT, the two-stage optimisation-based planner it was trained to imitate. Additionally, we present an ablation study which compares the output of the imitation learning network $\mathcal{N}_\theta^{2s\text{-OPT}}$ and alternatives as initialisations to the NLP solver.

A. Setup

We follow the implementation in [4] for 2s-OPT, and take the second stage (NLP) as the efficient optimiser ν in PILOT, implemented using IPOPT [28].

The first experiment uses a training dataset of 70,000 procedurally-generated problems of two-lane, urban driving in a residential setting. The problems are generated from 33 manually-designed base scenarios that contain a mixture of static and moving vehicles. The ego vehicle's position, heading and speed are perturbed at different timesteps of the original scenarios to create new configurations. Each of these configurations is considered a planning problem and solved by 2s-OPT, creating a high-quality expert dataset. We use an 80-20 split for training and testing datasets, respectively.

After initial training of the neural network, the training dataset is augmented with new problems generated interactively by PILOT when used in a driving simulator in new problems similar to the ones in the dataset. The new problems are solved by 2s-OPT as well to provide the expert trajectories. In a DAgger fashion, we add 64 new problems to the training dataset every training epoch.

The second experiment uses the CARLA simulator [25] where we generated 20,604 planning instances by running a baseline planner in 12-second, randomly-generated scenarios in Town02, collected problem instances at a rate of 1.5 Hz, and computed their 2s-OPT solutions, to pre-train PILOT. Then we run DAgger training on Town02 using the CARLA simulator and CARLA's Autopilot to control up to 40 randomly-spawned non-ego agents. We benchmark PILOT on a dataset generated in Town01 using 2s-OPT.

B. Results

We report results on the quality of PILOT when compared to 2s-OPT using two metrics:

- *Solving time* – the time required to initialise the NLP stage (i.e. using the MILP stage in 2s-OPT and using the neural network in PILOT), run NLP, and the total time. Lower solving time is better.
- *Cost* – the cost of the output of the NLP stage upon convergence as defined in Eq. 2. This reflects the quality of the solution, where lower final cost values are better.

The values are reported as *mean \pm standard deviation*. We report these metrics for the procedurally-generated experi-

TABLE I
SOLVING TIME AND QUALITY ON BENCHMARKING PROBLEMS

Planner	Time (s)			Cost
	Initialisation	NLP	Total	
PILOT	0.02 ± 0.00	0.23 ± 0.37	0.25 ± 0.37	1.10 ± 1.32
2s-OPT	0.86 ± 2.88	0.30 ± 0.89	1.16 ± 3.01	1.07 ± 1.16

(a) The procedurally-generated experiment on 945 problems where both PILOT and 2s-OPT converged.

Planner	Time (s)			Cost
	Initialisation	NLP	Total	
PILOT	0.01 ± 0.00	0.11 ± 0.18	0.13 ± 0.18	0.56 ± 0.68
2s-OPT	0.64 ± 1.22	0.16 ± 0.21	0.81 ± 1.27	0.54 ± 0.67

(b) CARLA experiment on 929 problems where both PILOT and 2s-OPT converged.

ment and for the CARLA experiment by randomly sampling a benchmarking set of 1,000 problems from the respective test dataset and computing the two metrics in problems successfully solved by both PILOT and 2s-OPT. The results for the procedurally-generated experiment are shown in Table I(a), and for the CARLA experiment in Table I(b).

These results vindicate our approach of combining an imitation learning with an optimisation stage, resulting in an efficient approach to planning safe and comfortable trajectories. As the results show, PILOT shows a clear advantage in runtime efficiency (saving of $\sim 78\%$ and 84% respectively) with no significant deterioration in solution quality (drop of $\sim 3\%$ and 4% respectively). By testing in a different town than the one in the training examples in the CARLA experiment, we show our framework has at least reasonably generalised to this new environment.

Next, we present an ablation study on the quality of the imitation learning network as an initialisation to the NLP stage compared to alternatives. We use the same benchmarking problems from the procedurally-generated experiment above. The alternative initialisations we compare against include: **None** initialisation which sets ego state to zero at all timesteps; **ConstVel** a constant velocity initialisation that maintains a constant yaw; and **ConstAccel/ConstDecel** constant acceleration and deceleration initialisations are similar but the speed is changed with a constant rate until it reaches the allowed speed limit or 0, respectively. We compare these alternatives relative to the original MILP initialisation of 2s-OPT, as a baseline. We use three metrics:

- *Percentage of solved problems* – constrained, non-linear optimisation in general is not guaranteed to converge to a feasible solution, hence the quality of an initialisation would be reflected in a higher percentage of solved problems. We report the percentage of solved problems out of the problems that 2s-OPT solved.
- Δ *NLP solving time* – we report the average difference in solving time (relative to MILP) in the problems that both the initialisation method and 2s-OPT solved.

TABLE II
INITIALISATION ABLATION - NLP COMPARISON RELATIVE TO 2S-OPT
ON AVERAGE SOLVING TIME AND FINAL NLP COST (IN PROBLEMS
SOLVED BY 2S-OPT AND THE PARTICULAR INITIALISATION) AND
CONVERGENCE PERCENTAGE.

Initialisation	Δ NLP solving time (s)	Δ NLP cost (%)	Converged (%)
None	-0.00	+10.7%	97%
ConstVel	-0.29	+10.8%	91%
ConstAccel	-0.16	+0.0%	86%
ConstDecel	-0.34	+17.0%	93%
$\mathcal{N}_\theta^{2s\text{-OPT}}$ (PILOT)	-0.91	+0.9%	95%
MILP (2s-OPT)	-	-	100%

- Δ *NLP cost* – for problems solved by the initialisation method and 2s-OPT, we report the percentage change in the cost of the output trajectory compared to MILP.

The results are shown in Table II.

As the results show, PILOT’s neural network initialisation produces trajectories that are easier to optimise (as reflected in the reduction in NLP solving time) with a small increase in the final cost on average when compared to the MILP initialisation of 2s-OPT. One of the alternatives (ConstAccel) has a slight advantage in final NLP cost, but it takes more time when it converges and it fails to converge in 9% more examples to a solution.

V. RELATED WORK

Previous work looked into transferring knowledge by imitation learning from a better-informed expert to a network that does not have access to the same rich input as the expert at inference time [7], [9], [24], [32]. In our setting, the expert and the learner share the same problem specification, but differ in runtime requirements.

While there are several works on imitation learning of optimisation, e.g. [33], [34], most of them suggest end-to-end learning approaches that do not include an optimisation stage at runtime. Given the safety-critical nature of autonomous driving, we believe this is an important requirement of any deployed system, as it allows the system to potentially recover from issues with the learnt network.

In [21], Sun *et al.* suggest a learning framework to imitate a long horizon Model Predictive Control (MPC) optimisation-based approach, which is then used at inference time to define the cost function of a short horizon one. In this case, the short-term MPC problem is highly conditioned on the network’s output, which has the potential to create suboptimal solutions if the network yields a poor result.

Our approach poses no restrictions on the design of the optimisation objective that we wish the planner output to respect, while in settings such as [23] the optimisation problem should be carefully designed to ensure that the optimisation constraints are differentiable in order for them to be usable to train a planner network.

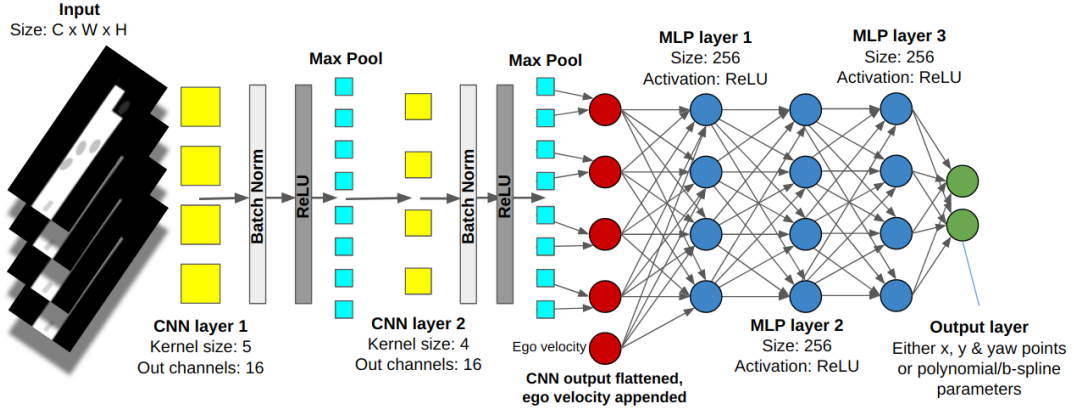


Fig. 4. PILOT network architecture

Bertsimas *et al.* [35] attempt an alternative approach to utilising the benefits of optimisation-based methods online, using machine learning to accelerate solving specific classes of Mixed-Integer Quadratic Programming problems. While this could work for the specific case of 2s-OPT, our approach poses no restrictions on the design of the optimisation problem and is thus more general.

VI. CONCLUSION

We present PILOT, an efficient and lightweight planning framework for autonomous driving, built with imitation learning and optimisation components, to produce plans with quality comparable to the planner it is based on. We employ imitation learning offline to imitate the output of an expensive-to-run optimisation-based planner. A constrained optimisation stage ensures, online, that the output of the network is feasible and conforms to various constraints related to road rules, safety and passenger comfort.

One drawback of using NLP optimisation is in convergence guarantees. Nonetheless, an advantage of having a light-weight solution is that multiple planners could be run in parallel with different levels of soft constraints, providing a fall-back mechanism that always respects the hard constraints. We plan to explore this direction further in future work.

APPENDIX

A. Network architecture

Fig. 4 shows PILOT’s neural network architecture.

B. Nonlinear Programming problem constraints

- $|\delta_k| \leq \delta_{\max}$, where δ_{\max} is maximum allowed steering input
- $a_{\min} \leq a_k \leq a_{\max}$, where $[a_{\min}, a_{\max}]$ is the allowed range for acceleration/deceleration commands
- $|a_{k+1} - a_k| \leq \dot{a}_{\max}$, where \dot{a}_{\max} is the maximum allowed jerk
- $|\delta_{k+1} - \delta_k| \leq \dot{\delta}_{\max}$, where $\dot{\delta}_{\max}$ is the maximum allowed angular jerk
- $0 \leq v_{\min} \leq v_k \leq v_{\max}$, where v_{\min} is the minimum desired speed, and v_{\max} is the road’s speed limit.

- $R(\phi_k) (\alpha^T \circ [w/2 \ l/2]^T) + [x_k \ y_k]^T \in \mathcal{B}$ for all $\alpha \in \{[1 \ 1], [-1 \ 1], [-1 \ -1], [1 \ -1]\}$, where $R(\phi_k) \in SO(2)$ is the rotation matrix for ϕ_k , \circ is the element-wise product operator, (l, w) are the vehicle’s length and width respectively, and \mathcal{B} is the driveable surface.
- For all $\alpha \in \{[1 \ 1], [-1 \ 1], [-1 \ -1], [1 \ -1]\}$:

$$\begin{bmatrix} x_k^\alpha - x_k^i \\ y_k^\alpha - y_k^i \end{bmatrix}^T R(\phi_k)^T \begin{bmatrix} \frac{1}{a_k^i}^2 & 0 \\ 0 & \frac{1}{b_k^i}^2 \end{bmatrix} R(\phi_k) \begin{bmatrix} x_k^\alpha - x_k^i \\ y_k^\alpha - y_k^i \end{bmatrix} > 1$$

where (x_k^i, y_k^i) is the centre and (a_k^i, b_k^i) are the semi-major and semi-minor axes of an ellipse that inscribes road user i at time k , and $R(\phi_k^i) \in SO(2)$ is the rotation matrix for orientation ϕ_k^i .

The parameters of the optimisation are in Table III.

TABLE III
NLP WEIGHTS AND PARAMETERS

Parameter	Value	Parameter	Value
L	4.8 m	v_{\max}	10 m/s
δ_{\max}	0.45 rad/s	ω_δ	2.0
a_{\min}	-3 m/s ²	ω_x	0.1
a_{\max}	3 m/s ²	ω_v	2.5
\dot{a}_{\max}	0.5 m/s ³	ω_y	0.05
$\dot{\delta}_{\max}$	0.18 rad/s ²	ω_a	1.0
v_{\min}	0 m/s		

C. Output transformation checks

The network produces a sequence of spatial positions, and the rest of the required input of the optimiser are computed from that sequence. A number of checks of upper and lower limits are applied to tame abnormalities in the network output and to improve the input to the optimiser.

- Velocity limits: $v_k \in [0, v_{\max}]$
- Acceleration/Deceleration limits: $a_k \in [a_{\min}, a_{\max}]$
- Maximum jerk limit: $|a_{k+1} - a_k| \leq \dot{a}_{\max}$
- Maximum steering angle limit: $|\delta_k| \leq \delta_{\max}$
- Maximum angular jerk limit: $|\delta_{k+1} - \delta_k| \leq \dot{\delta}_{\max}$

REFERENCES

[1] I. Batkovic, M. Zanon, M. Ali, and P. Falcone, “Real-time constrained trajectory planning and vehicle control for proactive autonomous driving with road users,” in *2019 18th European Control Conference (ECC)*. IEEE, 2019, pp. 256–262.

[2] J. Chen, W. Zhan, and M. Tomizuka, “Autonomous driving motion planning with constrained iterative LQR,” *IEEE Transactions on Intelligent Vehicles*, vol. 4, no. 2, pp. 244–254, 2019.

[3] W. Schwarting, J. Alonso-Mora, L. Paull, S. Karaman, and D. Rus, “Safe nonlinear trajectory generation for parallel autonomy with a dynamic vehicle model,” *IEEE Transactions on Intelligent Transportation Systems*, vol. 19, no. 99, 2017.

[4] F. Eiras, M. Hawasly, S. V. Albrecht, and S. Ramamoorthy, “Two-stage optimization-based motion planner for safe urban driving,” *arXiv preprint arXiv:2002.02215*, 2020.

[5] A. Sadat, S. Casas, M. Ren, X. Wu, P. Dhawan, and R. Urtasun, “Perceive, predict, and plan: Safe motion planning through interpretable semantic representations,” *arXiv preprint arXiv:2008.05930*, 2020.

[6] M. Bojarski, D. Del Testa, D. Dworakowski, B. Firner, B. Flepp, P. Goyal, L. D. Jackel, M. Monfort, U. Muller, J. Zhang *et al.*, “End to end learning for self-driving cars,” *arXiv preprint arXiv:1604.07316*, 2016.

[7] Y. Pan, C.-A. Cheng, K. Saigol, K. Lee, X. Yan, E. A. Theodorou, and B. Boots, “Imitation learning for agile autonomous driving,” *The International Journal of Robotics Research*, vol. 39, no. 2-3, pp. 286–302, 2020.

[8] J. Hawke, R. Shen, C. Gurau, S. Sharma, D. Reda, N. Nikolov, P. Mazur, S. Micklthwaite, N. Griffiths, A. Shah *et al.*, “Urban driving with conditional imitation learning,” in *2020 IEEE International Conference on Robotics and Automation (ICRA)*. IEEE, 2020, pp. 251–257.

[9] D. Chen, B. Zhou, V. Koltun, and P. Krähenbühl, “Learning by cheating,” in *Conference on Robot Learning*. PMLR, 2020, pp. 66–75.

[10] B. Paden, M. Čáp, S. Z. Yong, D. Yershov, and E. Frazzoli, “A survey of motion planning and control techniques for self-driving urban vehicles,” *IEEE Transactions on intelligent vehicles*, vol. 1, no. 1, pp. 33–55, 2016.

[11] S. V. Albrecht, C. Brewitt, J. Wilhelm, F. Eiras, M. Dobre, and S. Ramamoorthy, “Integrating planning and interpretable goal recognition for autonomous driving,” *arXiv preprint arXiv:2002.02277*, 2020.

[12] J. A. DeCastro, K. Leung, N. Aréchiga, and M. Pavone, “Interpretable policies from formally-specified temporal properties,” 2020.

[13] D. A. Pomerleau, “Alvinn: An autonomous land vehicle in a neural network,” in *Advances in neural information processing systems*, 1989, pp. 305–313.

[14] F. Codevilla, E. Santana, A. M. López, and A. Gaidon, “Exploring the limitations of behavior cloning for autonomous driving,” in *Proceedings of the IEEE International Conference on Computer Vision*, 2019, pp. 9329–9338.

[15] A. Filos, P. Tigas, R. McAllister, N. Rhinehart, S. Levine, and Y. Gal, “Can autonomous vehicles identify, recover from, and adapt to distribution shifts?” in *International Conference on Machine Learning (ICML)*, 2020.

[16] S. Ross, G. Gordon, and D. Bagnell, “A reduction of imitation learning and structured prediction to no-regret online learning,” in *Proceedings of the fourteenth international conference on artificial intelligence and statistics*, 2011, pp. 627–635.

[17] M. Bansal, A. Krizhevsky, and A. Ogale, “Chaffeurnet: Learning to drive by imitating the best and synthesizing the worst,” *arXiv preprint arXiv:1812.03079*, 2018.

[18] M. Mirman, T. Gehr, and M. Vechev, “Differentiable abstract interpretation for provably robust neural networks,” in *International Conference on Machine Learning*, 2018, pp. 3578–3586.

[19] E. W. Ayers, F. Eiras, M. Hawasly, and I. Whiteside, “PaRoT: A practical framework for robust deep neural network training,” in *NASA Formal Methods*. Springer International Publishing, 2020, pp. 63–84.

[20] C. Liu, T. Arnon, C. Lazarus, C. Barrett, and M. J. Kochenderfer, “Algorithms for verifying deep neural networks,” *arXiv preprint arXiv:1903.06758*, 2019.

[21] L. Sun, C. Peng, W. Zhan, and M. Tomizuka, “A fast integrated planning and control framework for autonomous driving via imitation learning,” in *Dynamic Systems and Control Conference*, vol. 51913. American Society of Mechanical Engineers, 2018, p. V003T37A012.

[22] J. Chen, B. Yuan, and M. Tomizuka, “Deep imitation learning for autonomous driving in generic urban scenarios with enhanced safety,” in *2019 IEEE/RSJ International Conference on Intelligent Robots and Systems (IROS)*, 2019, pp. 2884–2890.

[23] W. Zhan, J. Li, Y. Hu, and M. Tomizuka, “Safe and feasible motion generation for autonomous driving via constrained policy net,” in *IECON 2017 - 43rd Annual Conference of the IEEE Industrial Electronics Society*, 2017, pp. 4588–4593.

[24] T. Tosun, E. Mitchell, B. Eisner, J. Huh, B. Lee, D. Lee, V. Isler, H. S. Seung, and D. Lee, “Pixels to plans: Learning non-prehensile manipulation by imitating a planner,” *arXiv preprint arXiv:1904.03260*, 2019.

[25] A. Dosovitskiy, G. Ros, F. Codevilla, A. Lopez, and V. Koltun, “CARLA: An open urban driving simulator,” *arXiv preprint arXiv:1711.03938*, 2017.

[26] C. A. Floudas and P. M. Pardalos, *State of the art in global optimization: computational methods and applications*. Springer Science & Business Media, 2013, vol. 7.

[27] J. Nocedal and S. Wright, *Numerical optimization*. Springer Science & Business Media, 2006.

[28] A. Wächter and L. T. Biegler, “On the implementation of an interior-point filter line-search algorithm for large-scale nonlinear programming,” *Mathematical programming*, vol. 106, no. 1, pp. 25–57, 2006.

[29] A. Zanelli, A. Domahidi, J. Jerez, and M. Morari, “Forces nlp: an efficient implementation of interior-point methods for multistage nonlinear nonconvex programs,” *International Journal of Control*, pp. 1–17, 2017.

[30] A. L. Friesen and P. Domingos, “Recursive decomposition for non-convex optimization,” *arXiv preprint arXiv:1611.02755*, 2016.

[31] T. S. Lembono, A. Paolillo, E. Pignat, and S. Calinon, “Memory of motion for warm-starting trajectory optimization,” *IEEE Robotics and Automation Letters*, vol. 5, no. 2, pp. 2594–2601, 2020.

[32] S. Choudhury, M. Bhardwaj, S. Arora, A. Kapoor, G. Ranade, S. Scherer, and D. Dey, “Data-driven planning via imitation learning,” *The International Journal of Robotics Research*, vol. 37, no. 13-14, pp. 1632–1672, 2018.

[33] K. Lee, K. Saigol, and E. A. Theodorou, “Safe end-to-end imitation learning for model predictive control,” *arXiv preprint arXiv:1803.10231*, 2018.

[34] Y. Pan, C.-A. Cheng, K. Saigol, K. Lee, X. Yan, E. Theodorou, and B. Boots, “Agile autonomous driving using end-to-end deep imitation learning,” *arXiv preprint arXiv:1709.07174*, 2017.

[35] D. Bertsimas and B. Stellato, “Online mixed-integer optimization in milliseconds,” *arXiv preprint arXiv:1907.02206*, 2019.